

# Modeling the Thermoproteaceae RNase P RNA

Patricia P. Chan,<sup>1</sup> James W. Brown<sup>2</sup> and Todd M. Lowe<sup>1,\*</sup>

<sup>1</sup>Department of Biomolecular Engineering, University of California Santa Cruz; Santa Cruz, CA USA; <sup>2</sup>Department of Microbiology, North Carolina State University; Raleigh, NC USA

**T**he RNA component of the RNase P complex is found throughout most branches of the tree of life and is principally responsible for removing the 5' leader sequence from pre-tRNA transcripts during tRNA maturation. RNase P RNA has a number of universal core features, however variations in sequence and structure found in homologs across the tree of life require multiple Rfam covariance search models to detect accurately. We describe a new Rfam search model to enable efficient detection of the diminutive archaeal Type T RNase P RNAs, which are missed by existing Rfam models. Using the new model, we establish effective score detection thresholds, and detect four new RNase P RNA genes in recently completed genomes from the crenarchaeal family Thermoproteaceae.

## Introduction

Ribonuclease P (RNase P) has been studied intensively for its role in removing the 5'-leaders from pre-tRNAs during maturation. This ribonucleoprotein complex includes one or more well-studied proteins which vary by phylogenetic domain, and has one catalytic RNA subunit in most species with the notable exceptions among land-plants, mitochondria, chloroplasts and a small number of thermophilic microbes. The RNase P RNA (RPR) is the most evolutionarily conserved subunit of this complex, with characteristic structural differences among bacteria, archaea and eukaryotes.<sup>1</sup> RPRs typically consist of two structural domains with separate functions: the specificity domain involved in substrate binding, and the

catalytic domain needed for enzymatic cleavage. The Rfam database classifies all known RPRs into four different families: nuclear RNase P from eukaryotes, types A or B RNase P from bacteria and archaeal RNase P.<sup>2</sup> Although grouped together by Rfam, archaeal RPRs can be further divided into the two distinct types A and M.<sup>3</sup> The structure of archaeal type A RPR closely resembles that of bacterial type A RPR, and is the most common archaeal form found in currently sequenced genomes. The type M archaeal RPR, by contrast, lacks highly conserved RNA stem-loop structures in both the specificity, and catalytic domains; it has been found within the euryarchaeal genera *Archaeoglobus*, *Methanocaldococcus*, *Methanococcus* and *Methanothermococcus*. A new, significantly shortened form of archaeal RPR, type T, was recently found in multiple species within the crenarchaeal clade Thermoproteaceae, adding a third distinct form to Archaea.<sup>4</sup> Due to the absence of most of the specificity domain in this variant, the existing Rfam archaeal covariance model fails to identify it. Here, we review the features of the archaeal type T RPR, and the development of a covariance model to identify this unusual, newly recognized form of the RNA. Using this Rfam model, we detected additional type T RPR genes in newly available Thermoproteaceae genomes. In the course of our survey of all archaeal genomes, we also unexpectedly identified a novel type M variant in the clade Archaeoglobaceae.

## Results and Discussion

**Common features of type T RNase P RNAs.** The shortened, type T form of

**Keywords:** RNase P, Archaea, tRNA processing, RNA catalysis, RNA secondary structure

Submitted: 05/01/12

Revised: 07/13/12

Accepted: 07/16/12

<http://dx.doi.org/10.4161/rna.21502>

\*Correspondence to: Todd M. Lowe; Email: [lowe@soe.ucsc.edu](mailto:lowe@soe.ucsc.edu)

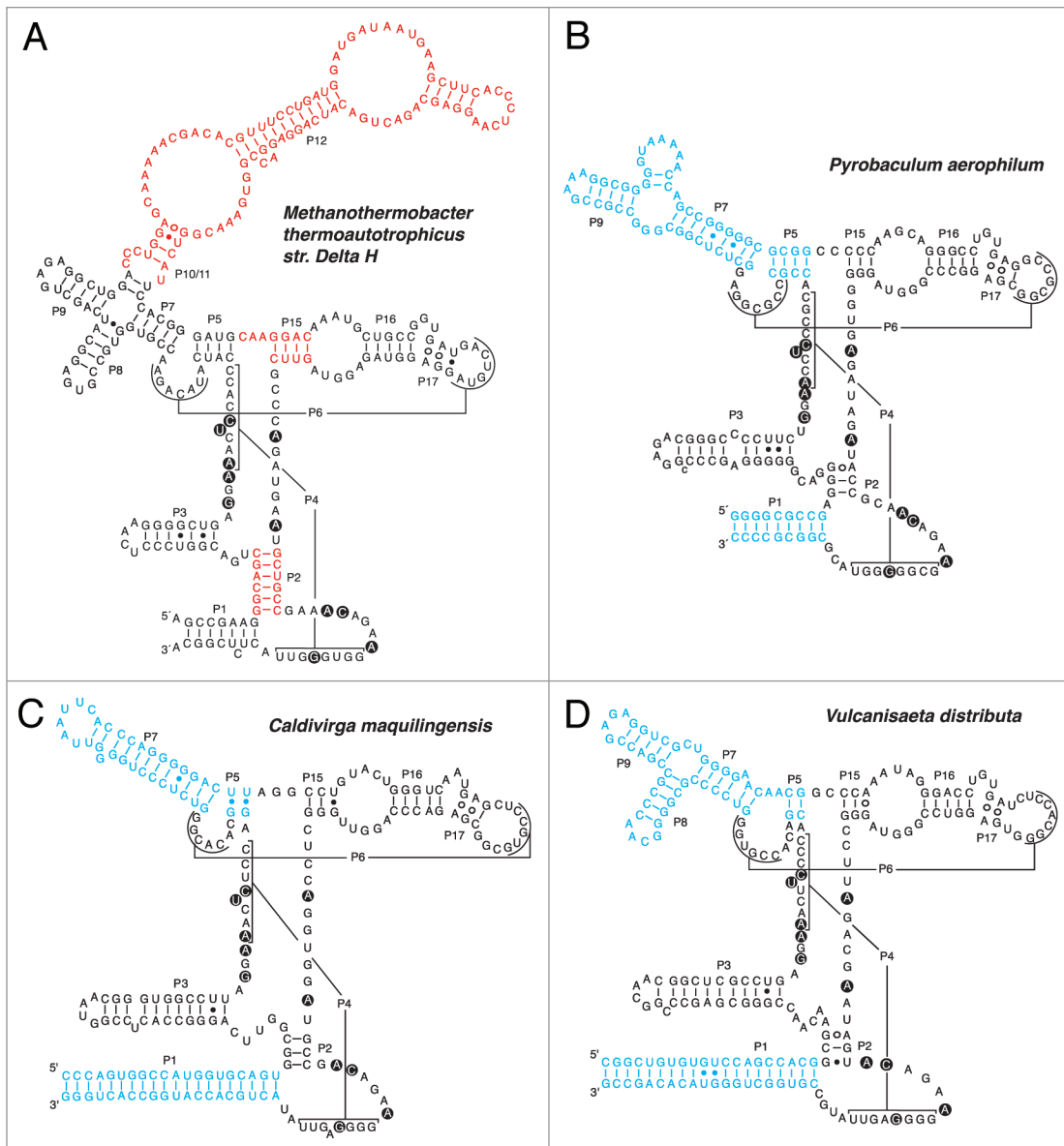


**Figure 1.** Predicted secondary structures of type T RNase P RNAs. (A) *Methanothermobacter thermoautotrophicus* RNase P RNA (RPR), a typical archaeal type A RPR, has both catalytic and specificity domains.<sup>3</sup> It is shown for comparison with type T RPRs. Common structural differences between type A and type T RPRs shown in red. Universally conserved nucleotides depicted by black circles—(B–D) Type T RPRs found in *Pyrobaculum aerophilum*, *Caldivirga maquilingensis* and *Vulcanisaeta distributa* have structural differences in P1, P5, P7, P8 and P9 stems, shown in blue.

RNase P RNA was recently described<sup>4</sup> in species of the genus *Pyrobaculum* (*P. aerophilum*, *P. arsenaticum*, *P. calidifontis*, *P. islandicum*, *P. oguniense* and *P. neutrophilum*), *Caldivirga maquilingensis*, and *Vulcanisaeta distributa*; all belong to the same phylogenetic family, Thermoproteaceae. In general, all type T RPRs have a catalytic domain closely resembling that of archaeal type A RPRs, but lack most of the specificity domain (Fig. 1). While the universally conserved positions in the P4 stem/

P4 joining region, and the P15/P2 joining region are present in type T RPRs, we note four specific differences that help to distinguish type T from other forms. First, the P2 stem is only 3 bp in length, which is relatively short compared with the 6 bp or 7 bp stems found in other archaea or bacteria, respectively.<sup>5</sup> Second, the P15 stem in all identified type T RPRs is 1 bp shorter than the typical P15 found in type A RPRs. Third, the 2-nt P5/P15 linker is contracted compared with the typical 3-nt linker usually found. Fourth, the P10 stem

that typically extends to P11, and P12 of the specificity domain in type A RPRs is terminated with a small loop (Fig. 1B and D) or is completely missing (Fig. 1C).

**Type T RNase P RNA variants.** Closer inspection of the secondary structures among the identified type T RPRs reveals three variants, one for each genus (Fig. 1). The 20-nt P1 stem in *C. maquilingensis* and *V. distributa* RNAs is about twice the length of those in *Pyrobaculum*. Although a long P1 stem has been observed in the predicted type A RPR of *Aeropyrum*

**Table 1.** Summary of RNase P RNA search results

Genome	Range of Covariance Model Search Score (bits)	
	Archaeal RNase P RNA Model (RF00373)	Archaeal Type T RNase P RNA Model
Thermoproteaceae	Not Detected – 10.20	117.04 – 168.79
Other archaea	53.55 – 228.58	Not Detected – 13.04
Virtual genomes with < 40% GC	Not Detected	Not Detected
Virtual genomes with about 50% GC	Not Detected – 14.34	Not Detected – 16.80
Virtual genomes with > 60% GC	Not Detected	Not Detected – 13.24

Infernal v1.0<sup>13</sup> cmsearch was used with the archaeal type T and existing Rfam<sup>2</sup> archaeal RPR covariance models to search archaeal genomes (Table S1) and 60 virtual genomes representing G/C content of < 40%, 50% and > 60%. Ranges of bit scores were reported. “Not Detected” indicates that no hits were identified when using default Infernal final score cutoff (0.0).

*pernix*,<sup>1</sup> the length of these type T members is among the longest in all verified archaeal RPRs. It was found in previous studies that P1 interacts with the terminal loop of P9 (L9) as part of the mechanism for orienting the catalytic, and specificity domains in bacterial RPRs.<sup>6,7</sup> A longer P1 stem that can contact L9 was found to significantly increase the catalytic activity of RNase P in *Methanothermobacter thermoautotrophicus*.<sup>8</sup> While both *Pyrobaculum* and *V. distributa* RPRs have a typical GNRA tetraloop in L9,<sup>6</sup> this tetraloop does not exist in *C. maquilingensis*' extended P7 stem (Fig. 1C), which has taken the place of P9 and P10. Thus, this atypical non-GNRA terminal loop may not serve to enhance catalytic activity in *C. maquilingensis*.

A typical P8 stem, similar to the one in archaeal type A RPRs, is only observed in *V. distributa*, but not in the other two variants (Fig. 1BD). P8 was found to be involved in T-loop recognition of pre-tRNAs in bacteria, mostly by interacting with L18 which is also absent in all archaeal RPRs.<sup>9,10</sup> The non-essentiality of P8 may be explained by recent studies demonstrating the replacement of the L18-P8 interaction by a protein-protein association and structural evidence for an indirect role of P8 in recognition of the T-loop<sup>11,12</sup>

A few other characteristics distinguish type T variants. The *C. maquilingensis* and *V. distributa* RNAs have the shortest P5 stem (2 bp vs. a typical 4 bp) observed in archaea. In addition, the *V. distributa* variant has a 2-nt joining region between P5 and P7, whereas other archaeal RPRs have no joining region.

**Searching with the type T covariance model.** A previously developed covariance

model built with only the *Pyrobaculum* RPR sequences does not perform well in searching for the two other type T variants.<sup>4</sup> This lack of generality is most likely due to the subtle differences in secondary structure noted above, as well as large disparity in G/C content between the *Pyrobaculum* RPRs (74–78%) vs. those found in *Caldivirga maquilingensis* (61%) and *Vulcanisaeta distributa* (66%). We therefore structurally aligned the RPR sequences from *Caldivirga maquilingensis*, *Vulcanisaeta distributa* and all six *Pyrobaculum* species to create a type T covariance model using Infernal<sup>13</sup> software.

To establish a false-positive score threshold for this model, we scanned 20 randomly generated genomes at each of 3 different G/C contents (< 40, 50 and > 60%). The maximum false positive scores for these were 0, 16.8 and 13.24 bits respectively. For comparison, we scanned the same randomly generated genomes with the existing Rfam archaeal RNase P covariance model and obtained scores within similar ranges (Table 1).

By employing this newly expanded model to new genomes, we identified four additional shortened forms of RPR, all within species in the Thermoproteaceae family: *Pyrobaculum sp* 1860, *Vulcanisaeta moutnovskia*, *Thermoproteus tenax* and *Thermoproteus uzoniensis* (Fig. 2; Data S1). The scores for these new identifications were close to the observed range for RPR sequences in the training set (124.2–167.0 bits; Data S2) and far exceeded the false positive threshold (16.8 bits), indicating that these are reliable new identifications. As expected, the RPRs in *P. sp* 1860 and *V. moutnovskia* have the same secondary structure, and

over 88% sequence identity when compared with other *Pyrobaculum* species and *V. distributa* (Fig. 2A and B). A partial RPR sequence fragment with a score of 33.61 bits was also detected in *P. sp* 1860, which is not similar to the high-scoring version found, so its origin is uncertain. Manual structural comparison shows that the RPRs in *T. uzoniensis* and *T. tenax* could be considered as *Pyrobaculum* type T variants, with sequence features highly similar to the *Pyrobaculum* orthologs (Fig. 2C and D). The 16S rRNA genes of *T. tenax* and *T. uzoniensis* place them closer to *Pyrobaculum* species (96%) than *C. maquilingensis* and *V. distributa* (93% and 94% respectively), consistent with the relative similarities of the new RPR genes. We also searched the *P. sp* 1860, *V. moutnovskia*, *T. tenax* and *T. uzoniensis* genomes with the existing Rfam archaeal covariance model to ensure there was only one RPR per genome and as expected, did not find any additional matches. A search for the RNase P proteins revealed likely homologs of Pop5, Rpp30 and Rpp29, but not Rpp21, as we previously observed for the other *Pyrobaculum* and *Vulcanisaeta* species,<sup>4</sup> further solidifying the genetic association of type T RPR and the conspicuous absence of Rpp21.

**Variations of P8.** Loss of the P8 stem in type M RPRs has been noted as one of the key structural differences distinguishing them from type A archaeal RPRs (Fig. 3A).<sup>3</sup> However, limited representation of RPRs from some archaeal clades necessarily allowed a limited assessment of the consistency of this feature among type M RPRs. While conducting structural comparisons between the type T and type M RPR genes, we identified a novel type M variant that includes a typical P8 stem

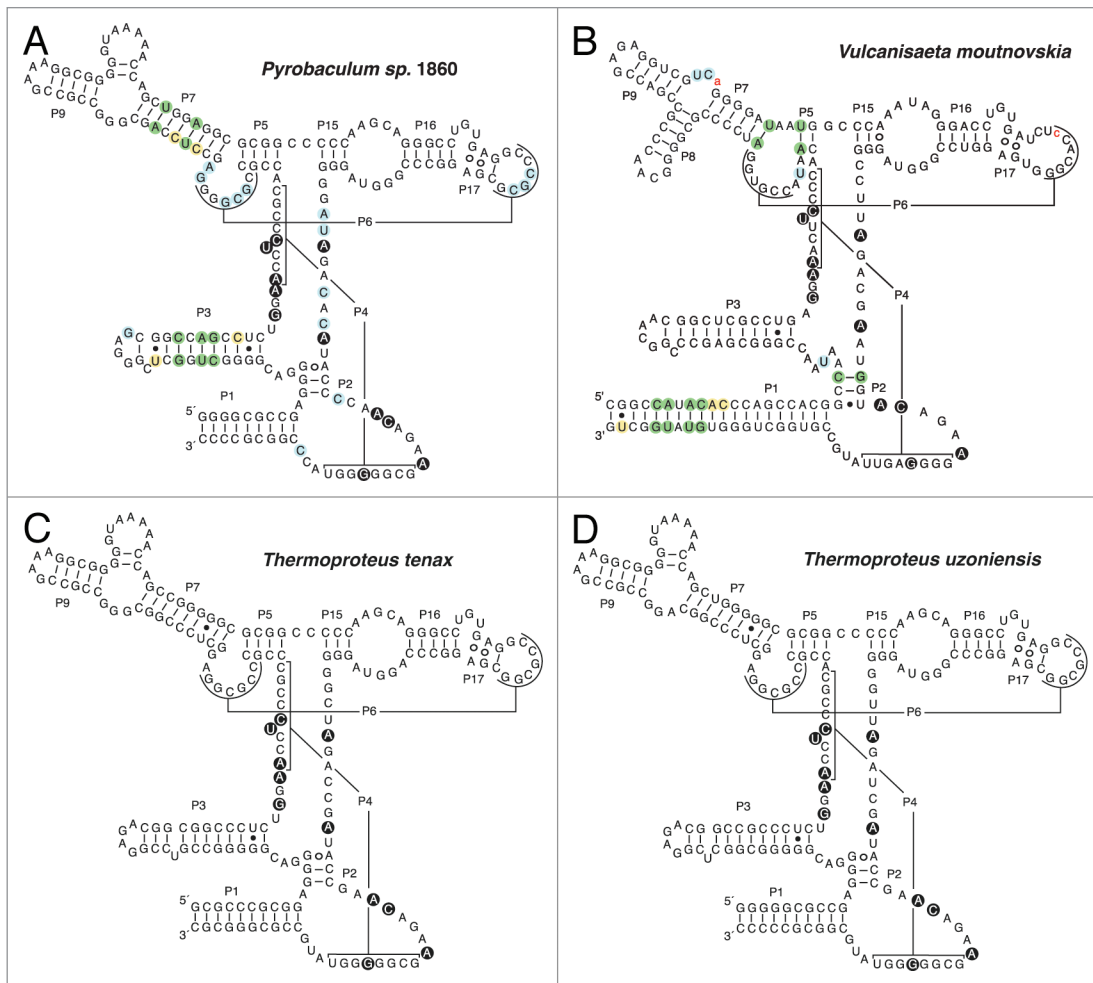


**Figure 2.** Predicted secondary structures of (A) *Pyrobaculum sp.* 1860, (B) *Vulcanisaeta moutnovskia*, (C) *Thermoproteus tenax* and (D) *Thermoproteus uzoniensis* RNase P RNAs (RPRs). (A and B). Black circles indicate universally conserved nucleotides. Other highlighted bases in *P. sp.* 1860 and *V. moutnovskia* are relative to other species in the same genus, *P. aerophilum* (Fig. 1B) and *V. distributa* (Fig. 1D), respectively. Annotated nucleotides show base pairing covariation (green), conservative G-C to G-U changes (yellow) and differences in unpaired regions (blue). Lower case red nucleotides show insertions or deletions between RPRs. (C and D) Predicted secondary structures of RPRs in *T. tenax* and *T. uzoniensis* resemble the *Pyrobaculum* type T RPR variant (Fig. 1B).

in three recently sequenced euryarchaea: *Archaeoglobus profundus*, *Archaeoglobus veneficus* and *Ferroglobus placidus*. This was not expected given that *Archaeoglobus fulgidus*, also belonging to the same phylogenetic family (Archaeoglobaceae), was previously found to lack the P8 stem and have a “typical” type M RPR.<sup>1,3</sup> Like the other type M RPRs, the genes in *A. profundus*, *A. veneficus* and *F. placidus* do not have L15, P16, P17 and P6 in their predicted structures. Yet, the presence of P8 in these species represents a novel combination of structural traits (Fig. 3B and C). The well-studied *A. fulgidus* now appears to be more similar in terms of RPR features to those found in methanogens and not as representative of RPRs

in the currently available members of the Archaeoglobaceae.

## Materials and Methods

**Genomic data.** Complete genomic sequences and annotated ORFs for all archaeal genomes were obtained from NCBI RefSeq.<sup>14</sup>

**Type T RNase P RNA covariance model development.** RNase P RNA sequences in *Pyrobaculum* (*P. aerophilum*, *P. arsenaticum*, *P. calidifontis*, *P. islandicum* and *P. neutrophilum*), *Caldivirga maquilungensis* and *Vulcanisaeta distributa* were aligned with the predicted secondary structures (Fig. 1) to enable manual creation of a structural alignment Stockholm

file. The programs cmbuild and cmcalibrate (Infernal v1.0<sup>13</sup> software package) took this file as input to build and calibrate the type T covariance model.

**Archaeal RNase P RNA sequence search.** The Infernal v1.0<sup>13</sup> program cmsearch was used to scan for RPR candidates in archaeal genomes using both the type T RPR covariance model and the existing Rfam<sup>2</sup> archaeal RPR covariance model (RF00373). Randomly generated genomes were scanned with the covariance models to determine the false positive score threshold. Six genomes (*Methanococcus maripaludis* S2, *Sulfolobus solfataricus*, *Pyrobaculum aerophilum*, *Methanothermobacter thermautotrophicus*, *Halogeometricum borinquense* and

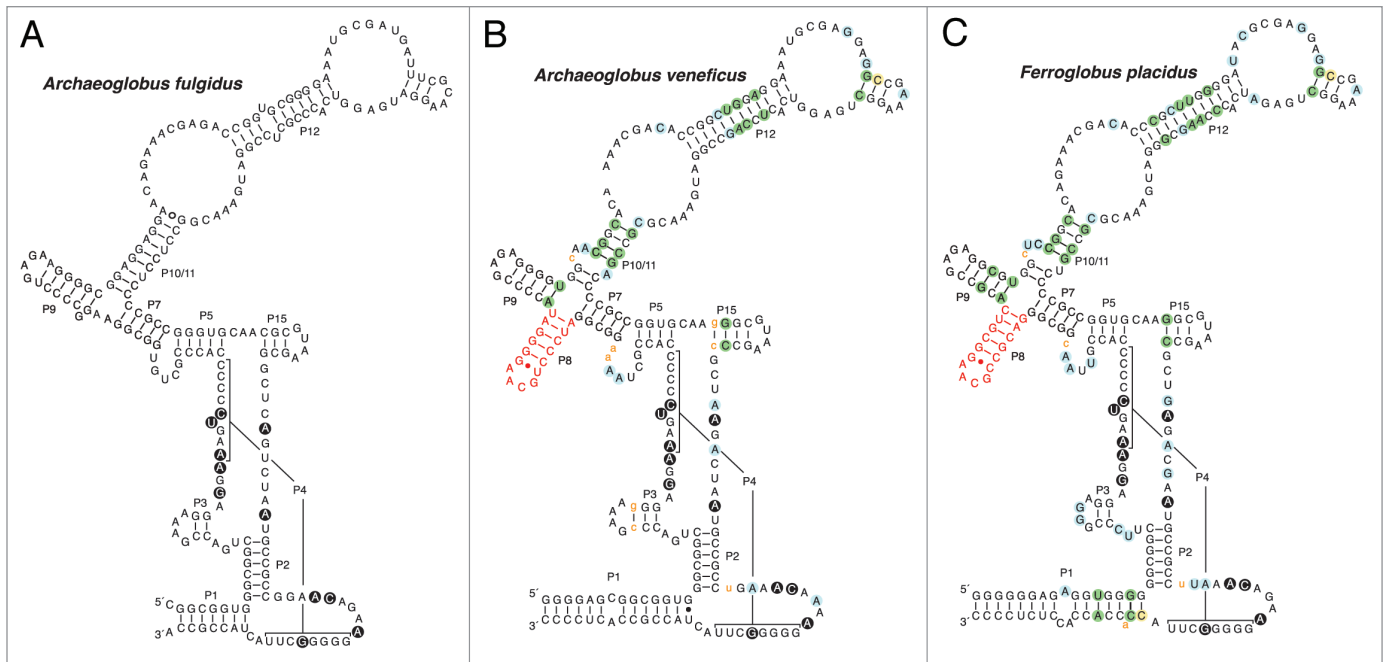


**Figure 3.** Predicted secondary structures of type M RNase P RNA variants. (A) *Archaeoglobus fulgidus* has a typical archaeal type M RNase P RNA (RPR) and is shown for comparison.<sup>3</sup> (B and C) Newly identified type M RPR variants in *Archaeoglobus veneficus* and *Ferroglobus placidus* have a P8 stem (red) that is missing in other type M RPRs. Other colored nucleotides are annotated as in Figure 2, indicating changes in (B and C) relative to (A).

*Methanopyrus kandleri*) that represent different G/C content (> 40%, 50%, < 60%) were selected as the basis for generating ten virtual genomes each using a 5th order Markov chain to retain the base hexamer frequencies of the target genomes. Cmssearch was initially run in the global search mode. All hits with a score greater than zero bits were manually examined. Local search mode was also employed, which provided better sensitivity but decreased selectivity.

RNase P protein database searches in *Pyrobaculum sp* 1860, *Vulcanisaeta moutnovskia*, *Thermoproteus tenax* and *Thermoproteus uzoniensis*. The protein sequences of Pop5, Rpp30, Rpp29 and Rpp21 for *P. sp* 1860, *V. moutnovskia*, *T. tenax* and *T. uzoniensis* were retrieved from Pfam<sup>15</sup> domain searches [RNase\_P\_Rpp14 (Pop5): PF01900; RNase\_P\_p30 (Rpp30): PF01876; UPF0086 (Rpp29): PF01868; and Rpr2 (Rpp21): PF04032]. Phylo-HMM<sup>16</sup> multiple alignments provided within the Archaeal Genome Browser<sup>17</sup> were used to predict synteny and orthology. Default scoring thresholds for PSI-BLAST (E-value: 10; word size: 3) and Pfam (trusted cutoff for Pop5: 23.4

bits; Rpp30: 20.3 bits; Rpp29: 21.1 bits; Rpp21: 23.2 bits) searches were initially adopted. Thresholds were further adjusted (E-value: 100 and word size: 2 for PSI-BLAST; trusted cutoff as -80 bits for Pfam) to search for proteins not identified with default search parameters.

## Conclusions

Type T RPRs in Thermoproteaceae display significant differences from the typical archaeal forms. Due to a lack of structural data, it is still an open question as to how this shortened RNA interacts with its protein subunits. The undetectable Rpp21 and the lack of most of the specificity domain leave open the possibility of one or more new subunits to be found, yet we were not able to identify computationally a separate specificity component (RNA or protein gene) encoded elsewhere in these genomes.<sup>4</sup> Determining the three dimensional structure of the holoenzyme and co-immunoprecipitation studies using known components may help address some of these uncertainties.

The discovery of multiple type T and type M RPR variants introduces a new

level of complexity to the architectural diversity of RNase P enzymes. The presence and absence of the P8 stem in different, closely related species suggests recent genetic swapping of RPR in *Archaeoglobus fulgidus* by lateral transfer. With the increasing availability of sequenced genomes, we anticipate that the new type T RPR model will help identify new variants for study and thus enable a more complete understanding of this dynamic RNA gene family.

## Disclosure of Potential Conflicts of Interest

No potential conflicts of interest were disclosed.

## Acknowledgments

This work was supported by National Science Foundation Grant EF-082277055.

## Supplemental Materials

Supplemental materials may be found here: [www.landesbioscience.com/journals/rnabiology/article/21502](http://www.landesbioscience.com/journals/rnabiology/article/21502)

## References

1. Brown JW. The Ribonuclease P Database. *Nucleic Acids Res* 1999; 27:314; PMID:9847214; <http://dx.doi.org/10.1093/nar/27.1.314>.
2. Gardner PP, Daub J, Tate J, Moore BL, Osuch IH, Griffiths-Jones S, et al. Rfam: Wikipedia, clans and the “decimal” release. *Nucleic Acids Res* 2011; 39(Database issue):D141-5; PMID:21062808; <http://dx.doi.org/10.1093/nar/gkq1129>.
3. Harris JK, Haas ES, Williams D, Frank DN, Brown JW. New insight into RNase P RNA structure from comparative analysis of the archaeal RNA. *RNA* 2001; 7:220-32; PMID:11233979; <http://dx.doi.org/10.1017/S1355838201001777>.
4. Lai LB, Chan PP, Cozen AE, Bernick DL, Brown JW, Gopalan V, et al. Discovery of a minimal form of RNase P in *Pyrobaculum*. *Proc Natl Acad Sci USA* 2010; 107:22493-8; PMID:21135215; <http://dx.doi.org/10.1073/pnas.1013969107>.
5. Haas ES, Armbruster DW, Vucson BM, Daniels CJ, Brown JW. Comparative analysis of ribonuclease P RNA structure in Archaea. *Nucleic Acids Res* 1996; 24:1252-9; PMID:8614627; <http://dx.doi.org/10.1093/nar/24.7.1252>.
6. Massire C, Jaeger L, Westhof E. Phylogenetic evidence for a new tertiary interaction in bacterial RNase P RNAs. *RNA* 1997; 3:553-6; PMID:9174090.
7. Massire C, Jaeger L, Westhof E. Derivation of the three-dimensional architecture of bacterial ribonuclease P RNAs from comparative sequence analysis. *J Mol Biol* 1998; 279:773-93; PMID:9642060; <http://dx.doi.org/10.1006/jmbi.1998.1797>.
8. Li D, Willkomm DK, Hartmann RK. Minor changes largely restore catalytic activity of archaeal RNase P RNA from *Methanothermobacter thermoautotrophicus*. *Nucleic Acids Res* 2009; 37:231-42; PMID:19036794; <http://dx.doi.org/10.1093/nar/gkn915>.
9. Nolan JM, Burke DH, Pace NR. Circularly permuted tRNAs as specific photoaffinity probes of ribonuclease P RNA structure. *Science* 1993; 261:762-5; PMID:7688143; <http://dx.doi.org/10.1126/science.7688143>.
10. Harris ME, Nolan JM, Malhotra A, Brown JW, Harvey SC, Pace NR. Use of photoaffinity crosslinking and molecular modeling to analyze the global architecture of ribonuclease P RNA. *EMBO J* 1994; 13:3953-63; PMID:7521297.
11. Li D, Gössringer M, Hartmann RK. Archaeal-bacterial chimeric RNase P RNAs: towards understanding RNA's architecture, function and evolution. *Chembiochem* 2011; 12:1536-43; PMID:21574237; <http://dx.doi.org/10.1002/cbic.201100054>.
12. Reiter NJ, Osterman A, Torres-Larios A, Swinger KK, Pan T, Mondragón A. Structure of a bacterial ribonuclease P holoenzyme in complex with tRNA. *Nature* 2010; 468:784-9; PMID:21076397; <http://dx.doi.org/10.1038/nature09516>.
13. Nawrocki EP, Kolbe DL, Eddy SR. Infernal 1.0: inference of RNA alignments. *Bioinformatics* 2009; 25:1335-7; PMID:19307242; <http://dx.doi.org/10.1093/bioinformatics/btp157>.
14. Pruitt KD, Tatusova T, Maglott DR. NCBI reference sequences (RefSeq): a curated non-redundant sequence database of genomes, transcripts and proteins. *Nucleic Acids Res* 2007; 35(Database issue):D61-5; PMID:17130148; <http://dx.doi.org/10.1093/nar/gkl842>.
15. Finn RD, Mistry J, Tate J, Coghill P, Heger A, Pollington JE, et al. The Pfam protein families database. *Nucleic Acids Res* 2010; 38(Database issue):D211-22; PMID:19920124; <http://dx.doi.org/10.1093/nar/gkp985>.
16. Siepel A, Haussler D. Combining phylogenetic and hidden Markov models in biosequence analysis. *J Comput Biol* 2004; 11:413-28; PMID:15285899; <http://dx.doi.org/10.1089/1066527041410472>.
17. Chan PP, Holmes AD, Smith AM, Tran D, Lowe TM. The UCSC Archaeal Genome Browser: 2012 update. *Nucleic Acids Res* 2012; 40(Database issue):D646-52; PMID:22080555; <http://dx.doi.org/10.1093/nar/gkr990>.